



Cite this: *Environ. Sci.: Water Res. Technol.*, 2025, 11, 306

## Emerging investigator series: Inactivation of antibiotic resistant bacteria and inhibition of horizontal resistance gene transfer is more effective by 222 than 254 nm UV†

Yijing Liu<sup>a</sup> and Natalie M. Hull  <sup>\*ab</sup>

The presence of antibiotic resistant bacteria (ARB) and the horizontal gene transfer (HGT) of antibiotic resistance genes (ARGs) in water environments pose a large and increasing threat to human health. This work compares the treatment efficiency of different ultraviolet (UV) wavelengths (222 nm KrCl excimer lamp and 254 nm low pressure Hg lamp) for inactivating multidrug antibiotic resistant *B. subtilis* strain 1A189, damaging its intracellular and extracellular ARGs, and inhibiting HGT of ARGs into non-resistant strain 1A1. The 222 nm wavelength was more effective than 254 nm at inactivation (dose required for 1 log reduction or  $D_1 = 4.11 \text{ mJ cm}^{-2}$  at 222 nm and  $8.99 \text{ mJ cm}^{-2}$  at 254 nm). ARG damage increased with dose and with increasing qPCR amplicon length for both UV wavelengths. Although extracellular ARG damage was similar between wavelengths, intracellular ARG damage was greater at 222 nm than 254 nm. Inhibition of HGT also increased with UV dose for both wavelengths, but was stronger at 222 nm for both extracted DNA ( $D_1 = 8.57 \text{ mJ cm}^{-2}$  at 222 nm and  $50.23 \text{ mJ cm}^{-2}$  at 254 nm) and intracellular DNA ( $D_1 = 20.14 \text{ mJ cm}^{-2}$  at 222 nm and  $92.90 \text{ mJ cm}^{-2}$  at 254 nm). When taking into account factors such as electrical efficiency and spectral absorbance that are less favorable for 222 nm, results showed that 222 nm was still more efficient at extracellular HGT inhibition, while 254 nm was more efficient for other assay endpoints. Overall, these comparisons demonstrate the superior mechanistic efficacy of 222 nm over 254 nm UV for disinfecting ARB and for inhibiting transfer of ARG despite similar ARG damage. This information will help inform and improve tools to address the global water challenge of antibiotic resistance to minimize risks to human health.

Received 24th June 2024,  
Accepted 31st October 2024

DOI: 10.1039/d4ew00530a

rsc.li/es-water

### Water impact

Ultraviolet (UV) disinfection at 222 nm is more effective than 254 nm at inactivating antibiotic resistant bacteria and inhibiting transfer of resistance genes. Although the novel 222 nm technology is limited by electrical efficiency, the efficacy of inhibiting gene transfer was still more efficient than 254 nm. These results enhance understanding of ARB treatment mechanisms toward optimizing UV for safe water.

## 1. Introduction

The presence of antibiotic resistant bacteria (ARB) and their antibiotic resistance genes (ARGs) jeopardize health by rendering antibiotics ineffective, thus posing risks for public health and ecosystems.<sup>1,2</sup> ARB are a prominent public health challenge of the 21st century, causing more than 23 000

deaths in the United States (US) and around 25 000 deaths in Europe annually in 2017 with enormous cost.<sup>3</sup> Deaths in the US increased to 35 000 in 2019.<sup>4</sup> ARB and ARG have the potential to transmit between humans, animals and throughout ecosystems.<sup>5,6</sup> ARB have been detected in a variety of environments including soils, streams, lakes, rivers, and coastlines.<sup>7,8</sup> Concerns about the microbial quality of water and transmission of ARB in water environments resulting in human exposure<sup>9</sup> have led to investigations of the presence and removal of ARB and ARG in engineered water systems.

ARB have been detected in wastewater treatment plant (WWTP) influents, activated sludge, effluents, and biofilms,<sup>10,11</sup> and the transfer of ARGs among bacteria can

<sup>a</sup> College of Engineering, Department of Civil, Environmental and Geodetic Engineering, The Ohio State University, Columbus, OH 43210, USA.

E-mail: hull.305@osu.edu, nataliehull@boisestate.edu

<sup>b</sup> The Sustainability Institute, The Ohio State University, Columbus, OH, 43210, USA

† Electronic supplementary information (ESI) available. See DOI: <https://doi.org/10.1039/d4ew00530a>

occur in the environment even after disinfection.<sup>12–14</sup> The selection pressure of engineered treatments, combined with the overuse of antibiotics, can promote the evolution of bacteria through both spontaneous mutation to confer resistant genes, and the spread of resistance genes among microbial communities through mechanisms such as horizontal gene transfer (HGT).<sup>15–17</sup> Previous studies have indicated that the environment of WWTPs can be beneficial for the growth of ARB and can increase the likelihood of gene transfer.<sup>10,18</sup> A review about the fate of ARB in WWTPs indicated that raw and treated wastewater exhibit a greater prevalence of ARB than surface water.<sup>18</sup> In other studies, highly abundant ARB were detected in both influent and effluent of a WWTP after chlorine disinfection.<sup>19–21</sup> ARB and ARGs have been detected in untreated drinking water sources, as well as in tap and bottled water.<sup>22,23</sup> Water distribution systems can allow proliferation of ARB and dissemination of ARG, resulting in higher quantities of ARGs in tap water than in both finished water and source water.<sup>24</sup>

Despite the prevalent detection of ARB and ARGs, disinfection has shown some efficacy in reducing ARB and ARGs in water sources and can serve as a protective barrier to restrict the proliferation and dissemination of ARB and ARGs.<sup>13,25,26</sup> However, field studies indicated that these methods cannot completely eliminate all resistant bacteria and genes, leading to potential dissemination into the environment.<sup>16</sup> Thus, the mechanisms of HGT inhibition and disinfection of ARB needs to be further explored. Research findings indicate the effectiveness of different disinfection processes (chlorine, UV irradiation, and peracetic acid) and ARB with different resistances to disinfectants.<sup>27</sup> Chlorination is one of the most widely used drinking water disinfection techniques. However, chlorination can result in the formation of toxic disinfection by-products (DBPs) such as trihalomethanes and haloacetic acids.<sup>28</sup> Chlorination also may be selected for some ARGs and promote HGT from ARB to pathogens by inducing genetic mutations.<sup>12,22,29</sup> Therefore, a deeper understanding of the dynamics between disinfectant exposure and the development of resistance is crucial for inhibiting the dissemination of ARGs, refining water treatment practices, and minimizing the risk of antibiotic resistance propagation.

Compared with chlorination, UV produces less potentially toxic DBPs, damages nucleic acids which can inhibit HGT of ARGs, and inhibits ARG expression.<sup>30,31</sup> The germicidal effect of UV light on bacteria and viruses is primarily due to the formation of pyrimidine dimers in DNA.<sup>32</sup> These DNA lesions disrupt the normal structure and function of the genetic material, interfering with essential cellular processes and inhibiting the microorganism's ability to replicate and survive.<sup>33</sup> As a result, UV disinfection effectively deactivates microorganisms by damaging their DNA, making UV highly relevant for combatting genes that confer antibiotic resistance. For ten ARGs across various WWTPs, it was found that the WWTP utilizing UV light as a frequent disinfection method during tertiary treatment exhibited the lowest

prevalence for all ten ARGs.<sup>34</sup> However, other studies indicated low levels of removal of ARGs after UV disinfection.<sup>35,36</sup> Previous studies also investigated the direct influence of disinfection on ARB and ARGs and revealed that UV disinfection can substantially reduce ARB and ARGs.<sup>2,19,37,38</sup> A recent study evaluated the performance of a 254 nm low pressure (LP) Hg lamp to disinfect ARB and ARGs in swine wastewater and indicated variable removal efficiencies for different ARGs,<sup>39</sup> indicating that more studies are needed to fully understand the impacts of UV on ARB and ARG.

LP Hg lamps emitting primarily 254 nm UV are commonly applied, but little is known about ARB disinfection, ARG damage, and HGT inhibition by other UV light sources and wavelengths. One alternative UV source is krypton-chloride excimer (KrCl) lamps, which have long lifetimes and mercury-free materials, and compared with LP Hg lamps they exhibit much fewer adverse effects on skin and eyes.<sup>40</sup> 222 nm UV is becoming highly relevant due to its enhanced efficacy for disinfection and general water treatment. For example, many organic micropollutants have higher photolysis rate constants and quantum yields at 222 nm than at 254 nm.<sup>41</sup> Additionally, 222 nm has been shown to be more efficient than 254 nm in a study inactivating *B. subtilis* spores due to triplet energy transfer from dipicolinic acid (DPA) to thymine bases.<sup>42</sup>

This work was therefore undertaken to compare kinetic dose response parameters for two different UV wavelengths (254 nm and 222 nm) for disinfecting *B. subtilis* ARB, and for damaging and inhibiting HGT of their ARGs to inform optimal wavelength options to inactivate and prevent the spread of ARB and ARGs and therefore minimize risks. By understanding the UV wavelength specific impacts for disinfecting ARB and for damaging and inhibiting transfer of ARGs, UV-based disinfection in water treatment systems can be optimized to protect public and environmental health.

## 2. Materials and methods

The overall study design was adapted from a previous study that focused on LP UV and other water treatments<sup>43</sup> to additionally compare 222 nm wavelength dependent dose responses for: disinfection of ARB using culture assays, damage of ARGs using molecular qPCR assays, and inhibition of HGT of ARGs using transformation assays. Additionally, the impact on ARG damage and HGT inhibition was compared for intracellular ARGs in cells *versus* extracellular ARGs in DNA extracted from cells before UV exposure. Finally, electrical efficiency was additionally considered in addition to mechanistic efficacy.

### 2.1 Bacterial strains and growth

*Bacillus subtilis*, a Gram-positive and spore-producing bacterium, was selected due to its various antimicrobial resistance phenotypes and mechanisms, carriers for exchanging ARGs, ease of cultivation, and extensive



availability of gene sequence data.<sup>43–45</sup> *Bacillus subtilis* strain 1A189 with chromosomal ARG (*blt*) was selected to be explored because it is a common multidrug transporter with broad substrate specificity.<sup>43,46</sup> *B. subtilis* strains 1A1 (nonresistant) and 1A189 (multidrug-resistant) were obtained from the Bacillus Genetic Stock Center (BGSC; Ohio State University). *B. subtilis* 1A189 exhibits a point mutation with an A–T base-pair deletion in the promoter region of the *blt* gene. The mutation conveys its resistance to multiple drugs. For incubation, 0.01 mL of each bacterial 25% glycerol stock was added with 6 mL antibiotic medium 3 growth medium (BD Difco™ Catalog No. DF0243-17-8, at pH 7) into an individual Erlenmeyer flask for 50 hours to monitor the OD<sub>600</sub> of the cell culture hourly, and then diluted in series with phosphate-buffered saline (PBS, Fisher BioReagents™ BP3991) to be plated in duplicate on nutrient agar (BD Difco™ DF0479-17-3) to determine its growth curve and timing of the exponential phase to be used for UV exposure (~26 hours). The growth curves of *B. subtilis* 1A189 and *B. subtilis* 1A1 are shown in Fig. S1 and S2.† PBS was used as the negative control.

## 2.2 DNA extraction

After culturing *B. subtilis* to the late exponential growth phase, DNA of *B. subtilis* strains 1A189 was extracted using a method with fewer steps and quicker turnaround than the protocol He *et al.* used,<sup>43</sup> modifying a previous protocol<sup>47</sup> using phenol:chloroform:isoamyl alcohol instead of phenol:chloroform. 500  $\mu$ L exponential phase ( $\sim 10^8$  CFU  $\text{mL}^{-1}$ ) bacterial culture was loaded to 20 DNA extraction tubes for extraction, and DNA pellets were resuspended in 200  $\mu$ L Tris-EDTA solution and used for UV exposure in the extracellular DNA study. For the intracellular study, DNA was extracted from untreated and UV exposed cells by the same method.

## 2.3 Ultraviolet light sources

An LP Hg lamp emitting nearly monochromatic light at a peak wavelength of 254 nm and an unfiltered krypton-

chloride excimer (KrCl) lamp exhibiting a dominant peak at 222 nm were used as UV sources. Emission spectra (Ocean Optics HDX UV-vis spectroradiometer) for both lamps are shown in Fig. 1.

## 2.4 UV dose determination and exposure

UV dose ( $\text{mJ cm}^{-2}$ ) is determined using two key parameters: wavelength and total UV. Standardized UV dose calculations described by Bolton and Linden (2003) include adjustment of variables such as measured incident irradiance (International Light ILT-5000 radiometer) and determination of Petri factor to account for non-uniformity across the sample surface, distance from light to the sample surface, sample depth, polychromatic sample absorbance (Agilent Cary 4000 UV-vis spectrophotometer), divergence of light throughout the sample depth, reflection factor at peak wavelength, and polychromatic lamp emission (Ocean Optics HDX UV-vis Spectroradiometer, NIST-traceable) and polychromatic radiometer response to calculate sample exposure times to achieve pre-determined UV doses.<sup>48,49</sup> The protocol used is an open-source protocol.<sup>50</sup> 3 mL of exponential phase cells diluted to approximately  $10^7$  CFU  $\text{mL}^{-1}$ , or their extracted DNA (1 ng  $\mu\text{L}^{-1}$ ), were exposed to fluences of 0–160  $\text{mJ cm}^{-2}$ . UV experiments were conducted fully in the dark environment and samples were covered with aluminum foil to avoid photo repair before transferring samples or plating.  $\log_{10}$  inactivation of cells,  $\log_{10}$  gene damage, and  $\log_{10}$  HGT inhibition were calculated using eqn (1).

$$\text{LI} = \log_{10} \frac{N_0}{N} \quad (1)$$

where  $N_0$  is the cell density ( $\text{CFU mL}^{-1}$ ), copy numbers for each amplicon, or recipient cell density at 0  $\text{mJ cm}^{-2}$  and  $N$  is the cell density ( $\text{CFU mL}^{-1}$ ), copy numbers for each amplicon, or recipient cell density in selective media after exposure to different UV doses.

UV dose responses were modeled with a three-parameter log logistic model fitted to the disinfection data using the ‘drm’ function from the ‘drc’ package (Version 3.0-1) in R Studio<sup>51</sup> using eqn (2).

$$\text{LI} = c + \frac{d - c}{1 + \exp(b \times (\log \text{Flunce} - \log e))} \quad (2)$$

where LI is  $\log_{10}$  inactivation for cell inactivation or  $\log_{10}$  gene damage for qPCR quantification;  $b$  is the slope of the curve at the middle point ( $e$ );  $c$  is the minimum value that could be obtained at 0 dose which we set to 0 resulting in a 3-parameter rather than a 4-parameter model; and  $d$  is the maximum value. Statistically significant differences were determined by observation of non-overlapping standard deviations of parameters in the inactivation, gene damage, and HGT inhibition between wavelengths and amplicon lengths. Additionally,  $D_1$  and  $D_2$ , which are the UV doses needed to achieve 90% ( $1 \log_{10}$ ) or 99% ( $2 \log_{10}$ ) reduction, respectively, were calculated using modeled parameters and are summarized in Table S1.†

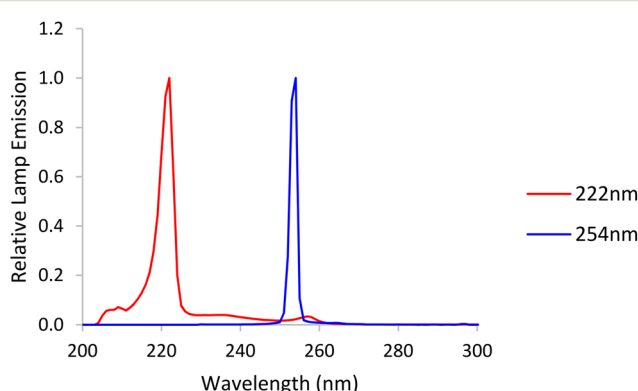


Fig. 1 Emission spectra from a low-pressure (LP) mercury lamp, labelled 254 nm, and a krypton-chloride excimer (KrCl\*) lamp, labelled 222 nm.



## 2.5 Gene damage

Quantitative polymerase chain reaction (qPCR) was used to measure the damage of the target chromosomal *blt* gene with four different amplicon lengths (1017 bp, 870 bp, 832 bp and 266 bp) through loss of ability to amplify. All qPCR tests were performed in triplicate on a QuantStudio 6 Flex Real-Time PCR System (Thermo Fisher Scientific, USA) with a total volume of 20  $\mu$ L, including 10  $\mu$ L SsoFast EvaGreen PCR Master Mix (Applied Biosystems, USA), 10  $\mu$ M forward and reverse primer, and 2  $\mu$ L template DNA. The cycling protocol for qPCR follows 40 cycles of denaturation at 94 °C for 20 s, annealing for 20 s and extension at 72 °C for 40 s.<sup>43</sup> Standard curves with gBlocks were used to calculate copy numbers. Sequences for each primer set and gBlocks were used without modification from a previous study.<sup>43</sup> The ARG damage efficiency was calculated using eqn (3).

$$LI = \log_{10} \frac{\text{Copy numbers after UV}}{\text{Copy numbers before UV}} \times 100\% \quad (3)$$

qPCR amplification efficiency for each amplicon size was derived from the slope of the standard curve for each primer set and was calculated using eqn (4); amplification efficiency for each amplicon was 98.5% (266 bp), 91.3% (832 bp), 95.4% (870 bp) and 92.6% (1017 bp).

$$E = \left( 10^{-\frac{1}{\text{slope}}} - 1 \right) \times 100\% \quad (4)$$

## 2.6 Horizontal gene transfer

Horizontal gene transfer of *B. subtilis* 1A189 DNA was quantified by natural transformation of the ARG into non-resistant *B. subtilis* 1A1 as described previously.<sup>43</sup> Transformation frequency was calculated as transformant cell density (CFU mL<sup>-1</sup>) measured on selective media (with 4 mg L<sup>-1</sup> acriflavine) over total recipient cell density (CFU mL<sup>-1</sup>) on nonselective media.

## 2.7 Electrical efficiency

Electrical energy per order (EEO, kW h m<sup>-3</sup> per order) represents the electric energy (kW h) required to remove the contaminant concentration per order of magnitude (90%) in 1 m<sup>3</sup> water. EEO was calculated as previously<sup>52</sup> according to the equation  $EEO = \frac{A \times D_N}{3.6 \times 10^6 \times V \times C \times WF}$ , where  $A$  is the irradiated surface area in cm<sup>2</sup> calculated using the diameter of the Petri dish (9.62 cm<sup>2</sup>).  $V$  is the sample volume in liters (0.003 L).  $D_N$  is the UV dose (mJ cm<sup>-2</sup>) required for obtaining a specific log reduction, which is the same as  $D_1$  or  $D_2$  for 1 or 2 log respectively, of cells or gene damage or HGT inhibition as summarized in Table S1.<sup>†</sup>  $C$  is the wall plug efficiency given by the manufacturer (0.35 for 254 nm (ref. 52) and 0.1 for 222 nm (ref. 53)).  $WF$  is the water factor, accounting for the UV absorbance and depth of the water, and we averaged the water factor from biological duplicate UV experiments. The factor  $3.6 \times 10^6$  converts between hours and seconds, mW and kW, and L and m<sup>3</sup>.

## 3. Results and discussion

### 3.1 ARB inactivation

To explore the effect of disinfection dose and compare the effects of different wavelengths on ARB, we investigated the inactivation of multidrug antibiotic resistant *B. subtilis* 1A189 from a UV dose of 0–160 mJ cm<sup>-2</sup>. Both 222 nm and 254 nm UV wavelengths disinfected *B. subtilis* 1A189 (Fig. 2). Parameters of the fitted log logistic model are available in Table S1.<sup>†</sup> The log<sub>10</sub> inactivation increased with increasing UV dose, but the 222 nm wavelength was more effective than 254 nm ( $D_1 = 4.11$  mJ cm<sup>-2</sup> at 222 nm and 8.99 mJ cm<sup>-2</sup> at 254 nm). The maximum observed inactivation was  $5.9 \pm 0.18$  log and  $5.38 \pm 0.01$  log at a dose of 160 mJ cm<sup>-2</sup> for 222 nm and 254 nm, respectively, for the initial concentration of *B. subtilis* of  $\sim 10^7$  CFU mL<sup>-1</sup>. At the UV dose of 40 mJ cm<sup>-2</sup> that is commonly applied in water treatment systems,<sup>54</sup>  $3.48 \pm 0.03$  and  $2.77 \pm 0.05$  log inactivation was observed for 222 nm and 254 nm, respectively.

In the study by He *et al.*,<sup>43</sup> the rate constant of ARB inactivation was fitted to a first order reaction and tailing occurred at around 25 mJ cm<sup>-2</sup>; 1 log reduction occurred around 5 mJ cm<sup>-2</sup> by 254 nm, which was slightly lower than our observation of 9 mJ cm<sup>-2</sup> required for 1 log reduction at 254 nm and slightly higher than 4 mJ cm<sup>-2</sup> required at 222 nm. Our findings align with previous research that demonstrated superiority of the KrCl excilamp over conventional Hg lamps for bactericidal efficacy against *Bacillus* spores<sup>55</sup> and bacterial endospores.<sup>56</sup> Similarly, a

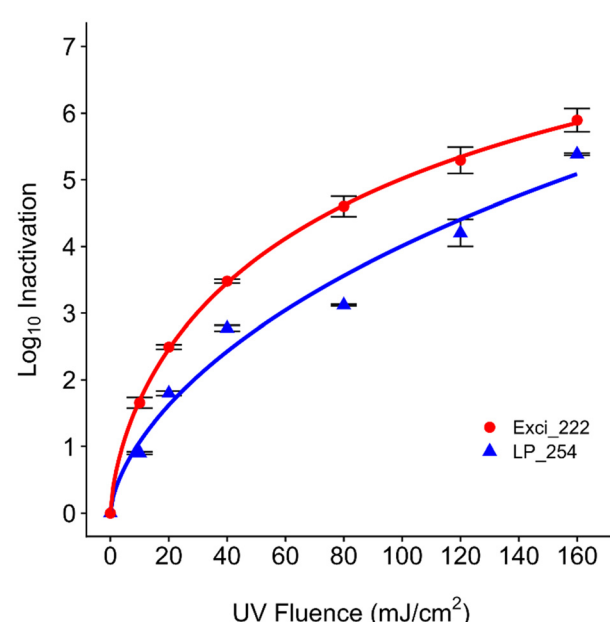


Fig. 2 UV dose response (222 nm, red circles vs. 254 nm, blue triangles) with the log logistic model (lines) for log<sub>10</sub> reduction of multidrug antibiotic resistant *B. subtilis* 1A189. Error bars represent the SEM of two averaged biological replicates, with three technical replicates each.



recent study applied 222 nm to disinfect waterborne pathogens and indicated the higher inactivation efficiency of *MS2*, *E. coli*, and *S. aureus* at 222 nm than 254 nm due to the damage of both proteins and nucleic acids.<sup>57</sup> Another study also indicated the higher inactivation efficiency of 222 nm over 254 nm on vegetative *B. subtilis*.<sup>55</sup> Differences in kinetics between wavelengths could be explained by previous studies which indicated higher inactivation of viruses at 222 nm over 254 nm due to more protein damage.<sup>58,59</sup> Proteins are more abundant in cells than nucleic acids, while 222 nm is more intensively absorbed by proteins which can cause photooxidation and cross-linking.<sup>55,60</sup> A study investigated different UV wavelengths (222 nm, 265 nm, and 285 nm) against chlorine-resistant bacteria and found 222 nm to promote the production of reactive oxygen species and cause cell membrane damage more than other wavelengths,<sup>61</sup> which may have contributed to higher inactivation at 222 nm in our study. Another study additionally explored other UV mechanisms rather than the formation of DNA lesions, indicating the effects of reactive oxygen species formation which 254 nm altered greatly compared to 222 nm.<sup>60</sup> However, in another study, higher disinfection performance at 254 nm than 222 nm on vegetative bacterial cells (*E. coli* K-12 and *M. smegmatis*) was observed in a thin-film aqueous solution,<sup>62</sup>

indicating potential differences across bacterial species and experimental setups and analyses or modeling that need to be further explored.

To contextualize these 254 nm UV doses within engineered systems and other ARB, one study in a municipal WWTP found that only 5 mJ cm<sup>-2</sup> was needed to obtain 1 log<sub>10</sub> inactivation of heterotrophic bacteria resistant to erythromycin and tetracycline,<sup>63</sup> which is much lower than the doses studied here. 1 log reduction in another study of multidrug-resistant *Pseudomonas aeruginosa* and vancomycin-resistant *Enterococcus faecium* required UV doses of only 2 and 8 mJ cm<sup>-2</sup>, respectively.<sup>38</sup> However, relative abundance of some ARB or ARGs increased after UV in WWTPs in some studies,<sup>16,32,63</sup> indicating possible differential selective pressure by UV on ARB. The regrowth of ARB was also observed after a UV dose of 10 mJ cm<sup>-2</sup>.<sup>64,65</sup> Recent studies have started exploring the impact of UV 222 nm on Gram-positive or Gram-negative bacteria, bacterial spores, and wastewater or drinking water samples<sup>61,66</sup> but have not focused specifically on ARB. Due to limited research on the specific impacts of UV wavelengths on ARB and the generally improved disinfection efficacy of 222 nm over 254 nm for several bacteria, these findings address the importance to further explore mechanisms of different UV wavelengths on other ARB and ARGs.

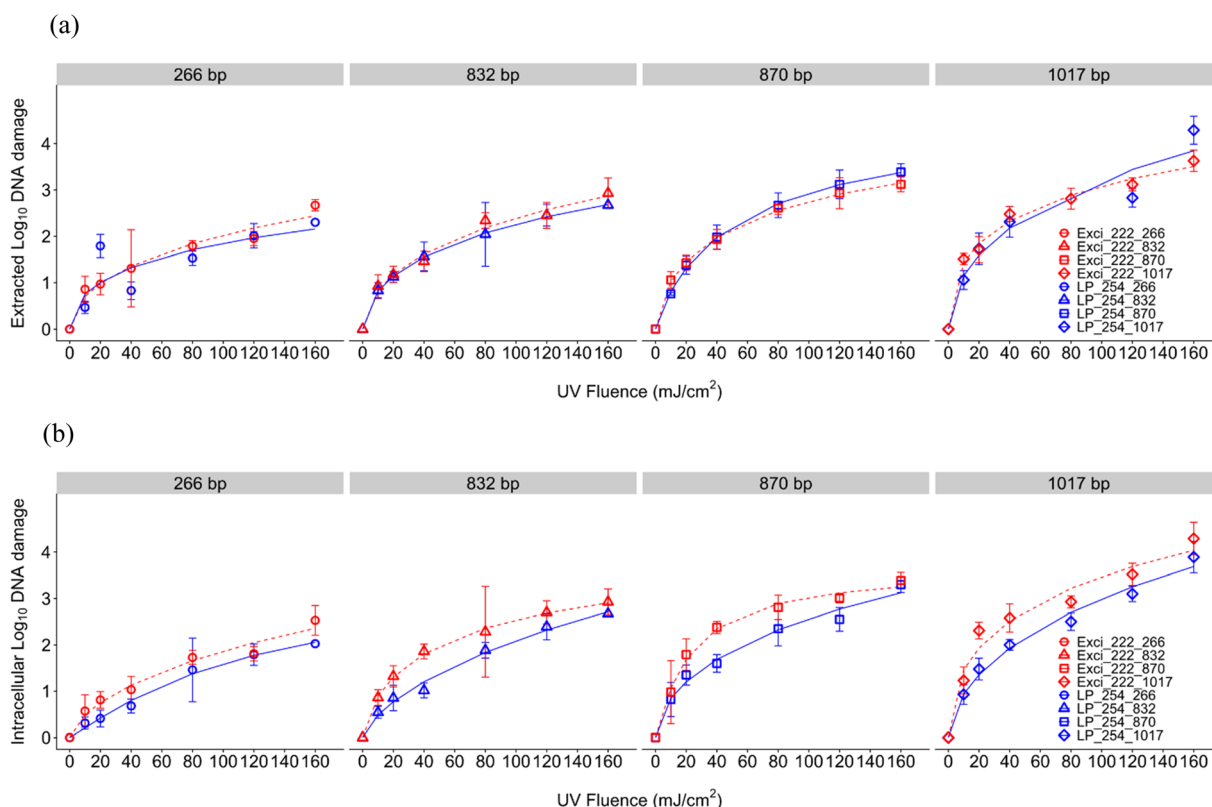


Fig. 3 UV dose response (222 nm, red vs. 254 nm, blue) with the log logistic model (lines) for log<sub>10</sub> (a) extracted and (b) intracellular DNA damage of increasing ARG amplicon lengths for a multidrug antibiotic resistant *B. subtilis* 1A189. Error bars represent the SEM of two averaged biological replicates, with three technical replicates each, at each UV dose.



### 3.2 ARG damage

For DNA damage of the *blt* gene conferring multidrug resistance to *B. subtilis*,  $\log_{10}$  DNA damage (calculated as the reduction of the ARG signal in qPCR) increased with UV dose for both UV wavelengths (Fig. 3). In general, shorter amplicons required a higher UV dose than longer amplicons to obtain the same reduction efficiency, which aligns with previous reports indicating the pattern of slower/lower ARG degradation using shorter qPCR amplicons<sup>43,67–71</sup> but contrasts a study that found no relationship with amplicon length.<sup>62</sup> This inverse relationship between amplicon length and loss of amplification is likely due to an increase in the number of nucleotides having more potential lesion targets. Compared to ARB inactivation, ARG damage was slower, which aligns with previous results.<sup>43,72</sup> The role of cell structure could be implicated in the study where no relationship between genome damage and amplicon length was observed because the high abundance of protein in cells may contribute to the increased absorbance of UV at 222 nm, resulting in relatively less bacterial genome damage compared to viruses.<sup>62</sup> A review identified ARGs in WWTPs and found that a significant reduction of ARB doesn't result in an efficient ARG removal, which could also explain the different rate constants between ARB and ARGs.<sup>73</sup> Our results show greater damage of this ARG than a previous study in drinking water where  $200 \text{ mJ cm}^{-2}$  resulted in incomplete elimination of ARGs (1.2 log reduction).<sup>64</sup>

For the extracted DNA, ARG damage efficiencies were comparable between 254 nm and 222 nm (Fig. 3, Table S1†). Because the UV absorption spectrum of DNA shows absorbance increasing below 220 nm and peaking at 260 nm,<sup>74</sup> the comparable ARG damage efficiencies of extracted DNA could be attributed to the fact that 254 nm and 222 nm have similar DNA absorbance when there are no other interfering or interacting compounds present. Due to limited interference of cellular materials or sample matrix components in solution, the impacts of which have been previously explored for 254 nm UV photoreactivity of nucleic acids,<sup>75</sup> extracted DNA damage may be attributed solely to direct UV absorption. Extracted DNA degradation at 254 nm seen here is comparable to the previous research that informed our study design.<sup>43</sup> Although He *et al.* used linear regression modeling including only UV doses up to  $45 \text{ mJ cm}^{-2}$  to exempt the tailing effect, we considered tailing by using the log logistic model. Due to the lack of sigmoidal shape, the linear rate constant in the log logistic model indicated by parameter *b* at the inflection point *e* doesn't adequately describe the gene damage kinetics alone, because the inflection point was sometimes at a dose greater than  $160 \text{ mJ cm}^{-2}$  (Table S1†). For more direct comparison to studies with linear dose responses, we calculated  $D_1$  and  $D_2$  for each amplicon length using fitted log logistic models, and took the inverse to determine rate constants  $k_1$  and  $k_2$  (Table S1†). The  $k_1$  and  $k_2$  for 254 nm for extracted DNA damage were  $0.050$  and  $0.011 \text{ cm}^2 \text{ mJ}^{-1}$  (266 bp),  $0.066$  and

$0.011 \text{ mJ cm}^2$  (832 bp),  $0.075$  and  $0.017 \text{ mJ cm}^{-2}$  (870 bp), and  $0.134$  and  $0.023 \text{ mJ cm}^{-2}$  (1017 bp). The  $k_1$  and  $k_2$  for 254 nm for intracellular DNA damage were  $0.019$  and  $0.066 \text{ cm}^2 \text{ mJ}^{-1}$  (266 bp),  $0.033$  and  $0.0109 \text{ mJ cm}^{-2}$  (832 bp),  $0.072$  and  $0.017 \text{ mJ cm}^{-2}$  (870 bp), and  $0.089$  and  $0.023 \text{ mJ cm}^{-2}$  (1017 bp). As can be seen from these rate constants, we observed a faster gene damage rate with extracted DNA than intracellular DNA. He *et al.*'s rate constants for extracted DNA damage ( $0.02$ – $0.088 \text{ mJ cm}^{-2}$ ) for 254 nm fell between our observed  $k_1$  and  $k_2$  values, and rate constants for intracellular DNA damage were consistent with the extracted DNA (2019). Our rate constants also indicate faster gene damage with increasing amplicon length after UV disinfection, which was also illustrated by previous studies.<sup>43,69,76</sup> In addition to different modeling, other slight differences from He *et al.* could be due to our differing experimental set up. We conducted collimated beam UV exposure experiments while they used a merry-go-round photoreactor, resulting in different reflection and divergence factors. The difference in reaction volume (3 ml Petri dish compared to 100 ml quartz tube) may have also affected kinetics due to different light penetration and therefore water factor.

Comparing between extracted and intracellular DNA damage, UV dose responses demonstrated slightly different patterns. In our study, intracellular DNA required higher doses to damage the ARG ( $D_1$ ) than extracted DNA as shown in Fig. 5(a) and Table S1†. However as can be seen when comparing dose responses, differences between modeled parameters were minimal with overlapping errors (Table S1†). Both extracted and intracellular DNA exhibited similar tailing (*d* parameter) for both wavelengths. Tailing has been observed after 254 nm previously,<sup>43</sup> and has been hypothesized to be due to combined effects of formation and photoreversal of CPD but irreversible formation of 6–4 photoproducts.<sup>77</sup> Since tailing parameters did not differ, wavelength impacts are likely minimal. These minimal impacts between extracted and intracellular ARG damage are supported by previous comparisons using two Gram-positive bacteria and two Gram-negative bacteria under 254 nm that indicated no significant differences between extracted DNA and intracellular gene damage.<sup>38</sup> No significant difference was observed in 254 nm UV degradation of intracellular DNA or extracted DNA in another study.<sup>78</sup> Another 254 nm study of *Acinetobacter* spp. showed similar deactivation rate constants of chromosomal methicillin-resistant *mecA*, but more tailing was observed in intracellular DNA,<sup>77</sup> while the tailing effects for extracted and intracellular DNA were similar in our study as indicated by parameter *d* (Table S1†). Results are also comparable to another study that treated two ARGs (~800 bps) at UV 254 nm; however intracellular ARGs had a slower rate of damage compared to extracted, with a key difference being that the ARG was encoded on a plasmid<sup>76</sup> rather than on chromosomes as studied here. A study with a plasmid encoded *amp* gene in *E. coli* indicated that  $37 \text{ mJ cm}^{-2}$  at 254 nm UV was required for  $1 \log_{10}$  reduction of both extracted and intracellular ARGs (Yoon,



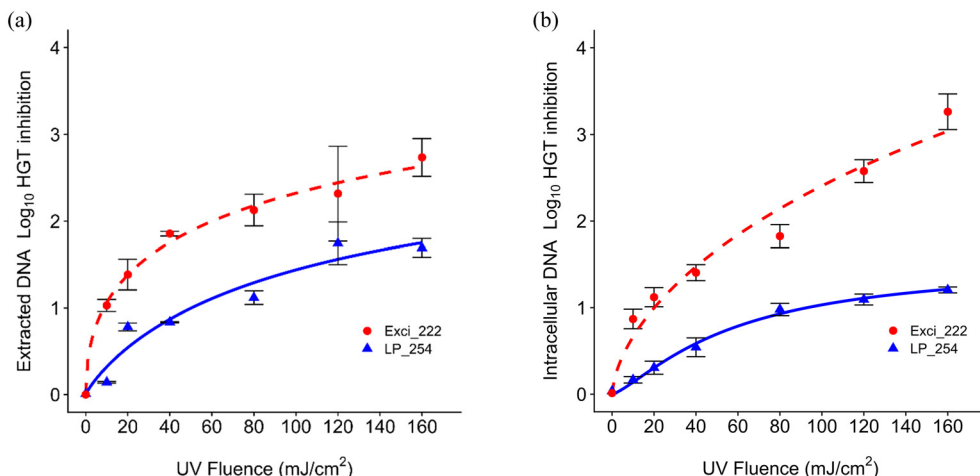


**Fig. 4** UV dose response (222 nm, red vs. 254 nm, blue) with the log logistic model (lines) for log<sub>10</sub> HGT inhibition after (a) extracted and (b) intracellular UV exposure. Error bars represent the SEM of three averaged biological replicates, with three technical replicates each, at each UV dose.

Dodd, and Lee 2018),<sup>69</sup> which was lower than the dose required in our study with a chromosomal ARG. Additionally, a recent investigation demonstrated that 254 nm UV treatment led to comparable rates of inactivation between extracellular and intracellular forms of chromosomal ARGs, but chromosomal ARGs degraded faster than plasmid ARGs.<sup>78</sup> Taken together these results and the literature indicate that further study may be warranted to discern the impact of UV wavelengths on damaging plasmid encoded ARGs.

### 3.3 ARG transfer inhibition

As shown in Fig. 4, the log<sub>10</sub> inhibition of *blt* gene HGT generally increased with UV dose. The dose responses show that 222 nm was more effective than 254 nm on HGT inhibition as shown by  $D_1$  in Table S1† for both extracted and intracellular DNA inhibition (extracted:  $D_1 = 8.57 \text{ mJ cm}^{-2}$  at 222 nm and  $50.23 \text{ mJ cm}^{-2}$  at 254 nm; intracellular:  $D_1 = 20.14 \text{ mJ cm}^{-2}$  at 222 nm and  $92.9 \text{ mJ cm}^{-2}$  at 254 nm). The rate constants for HGT inhibition were lower than those for both cell inactivation, which aligns with previous results.<sup>79</sup> Extracted DNA required lower doses than intracellular ARGs for HGT inhibition. The rate constants for HGT inhibition were similar to those for 266 bp and 832 bp ARG damage. He *et al.* also found that the HGT inhibition rate was similar to the gene damage for all amplicons, but was higher than the 260 bp gene damage.<sup>43</sup>

Previous work demonstrated that the rate constant of transforming plasmid encoded ARGs was lower than that of CPD formation under 254 nm UV.<sup>69</sup> Another study indicated that DNA integrity affecting the transformation and lower intracellular rate constant for transformation than that for gene damage may be due to gene repair.<sup>43</sup> Plasmid encoded ARGs exposed to UV LEDs at 265 nm and 285 nm at  $40 \text{ mJ cm}^{-2}$  or  $186 \text{ mJ cm}^{-2}$  indicated that 265

nm was more efficient than 285 nm on inhibiting gene damage and gene transfer.<sup>70</sup> No studies have explored the impacts of UV 222 nm on HGT. Our findings regarding more effective HGT inhibition at 222 nm could promote further exploration or application of 222 nm in water engineered systems.

### 3.4 Electrical energy comparisons

Comparisons of electrical energy per order, EEO, which is the electrical energy required for 1 log<sub>10</sub> cell inactivation, ARG damage, and HGT inhibition, are summarized in Fig. 5 along with the summary of  $D_1$  used to calculate the EEO for each condition. A lower EEO value indicates greater energy efficiency.<sup>80</sup> Most notably, EEO value for both extracted and intracellular HGT inhibition were higher for 254 nm LP than 222 nm KrCl, indicating that 222 nm is both more effective and more electrically efficient at preventing HGT of ARGs than 254 nm.

A similar EEO was required between wavelengths for 2 log extracted DNA HGT inhibition (Fig. S3†), but UV 222 nm required a lower dose ( $60.14 \text{ mJ cm}^{-2}$  for 222 nm and  $236.81 \text{ mJ cm}^{-2}$  for 254 nm). EEO is greatly impacted by having high wall plug efficiency (WPE) to use less energy for disinfection,<sup>81</sup> and the maximum WPE for 222 nm was lower than 254 nm. A competitive EEO was required between wavelengths for ARB inactivation as shown in Fig. 5b and S3b† ( $0.004$  (222 nm) and  $0.002$  (254 nm) kW h m<sup>-3</sup> for  $D_1$ ,  $0.013$  (222 nm) and  $0.008$  (254 nm) kW h m<sup>-3</sup> for  $D_2$ ). Although UV 222 nm had a lower WPE and water factor, UV 222 nm showed competitive energy efficiency on ARG damage. Our results align with another study about virus disinfection that indicated LP and excimer lamps to be competitive in terms of disinfection energy requirements.<sup>53</sup>

HGT inhibition had a similar EEO to ARG damage of shorter amplicons, and ARB disinfection had a similar EEO



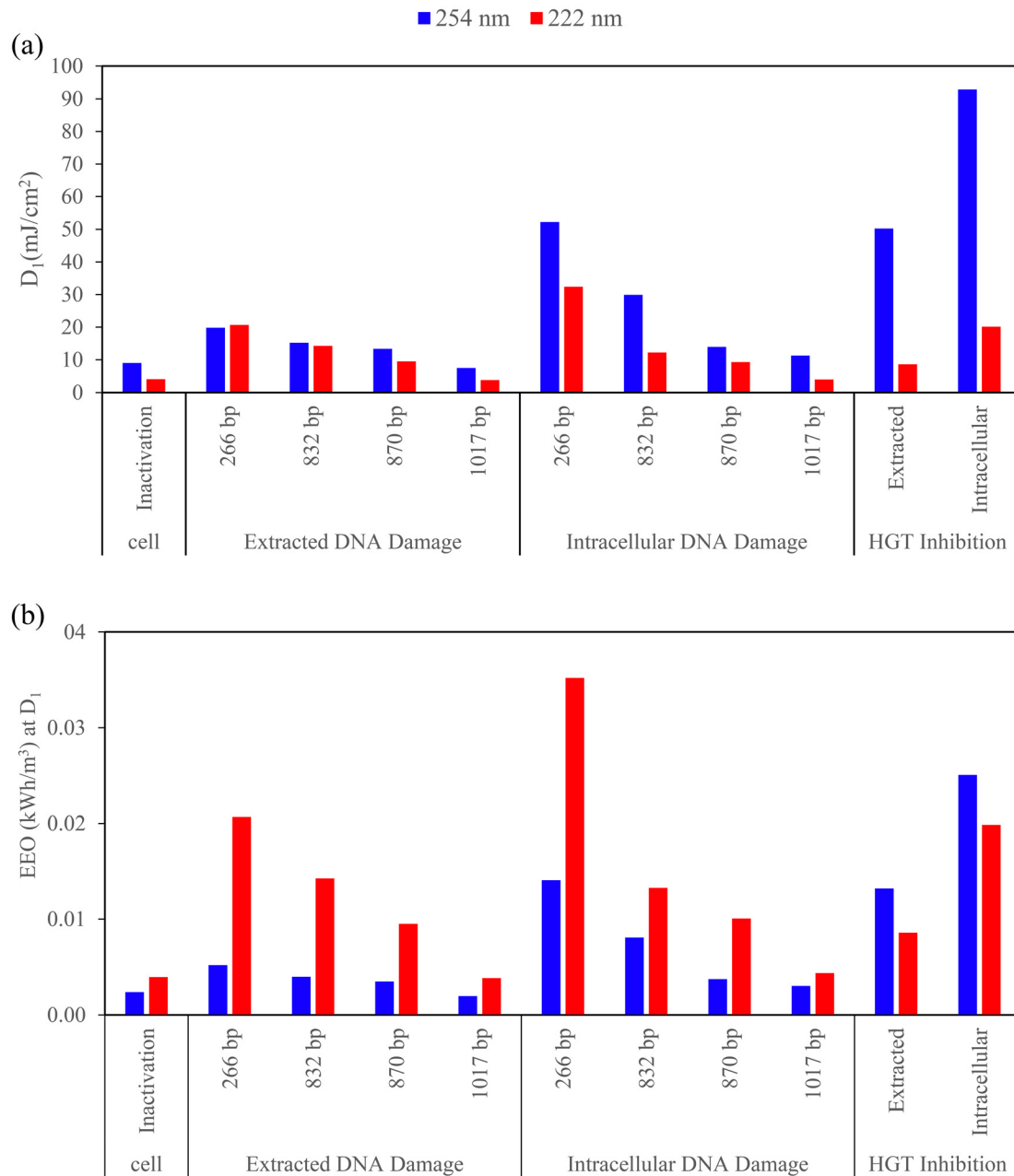


**Fig. 5** (a)  $D_1$  for  $1\log_{10}$  reduction and (b) electrical energy per order (EEO) at  $D_1$  of: cell inactivation, extracted DNA damage at various amplicon lengths, intracellular DNA damage at various amplicon lengths, and HGT inhibition of intracellular and extracted DNA with 254 nm (blue) and 222 nm (red) UV.

to ARG damage of longer amplicons. For ARG damage, shorter amplicons required higher energy than longer amplicons for both extracted and intracellular DNA at both UV wavelengths, which aligns with the lowered rate constants of damaging shorter amplicons. In general, for ARG damage, the EEO was higher for 222 nm and for intracellular DNA, but the variation was almost overlapped with 254 nm. Due to the nonlinearity of dose responses, differences were examined when comparing  $D_1$  and corresponding EEO (Fig. 5b) with  $D_2$  and corresponding EEO (Fig. S3b†). UV doses required for extracted DNA

damage with shorter amplicons were similar between 254 nm and 222 nm for  $D_1$ , but 222 nm was more effective than 254 nm when comparing  $D_2$ . The EEO values here for disinfection at 254 nm are within the range of those reported for *Escherichia coli*, MS2 coliphage, human adenovirus type 2, and *Bacillus pumilus* spores (0.006–0.297 kW h m<sup>-3</sup> for 2 log reduction at 254 nm).<sup>52</sup> In our study, 0.008 kW h m<sup>-3</sup> was required for 2 log reduction of *B. subtilis* at 254 nm while 222 nm required 0.013 kW h m<sup>-3</sup>. In their study, the EEO to obtain a 2 log reduction for *B. pumilus* was 0.297 kW h m<sup>-3</sup> using LP 254 nm and 0.373

## Paper

$\text{kW h m}^{-3}$  using MP which were higher compared with our study for *B. subtilis*, possibly due to resistance differences among *Bacillus* species. In their study, LP and MP UV lamps were more electrically efficient than UV LEDs. EEO also varied among different species in their study, where LP was the most efficient for inactivating *E. coli* and MS2 and MP and LP were equally efficient for inactivating HAdV2 and *B. pumilus*. More recently, the reported WPE and energy efficiency of LEDs are still low, WPEs of 0.003 (255 nm), 0.007 (265 nm) and 0.016 (285 nm) were applied to analyze the energy consumption of UV LEDs on P22 virus and *E. coli* and 255 nm had the lowest energy efficiency.<sup>82</sup> Another UV LED study with 265, 280 and 300 wavelength disinfected *Pseudomonas aeruginosa*, *Legionella pneumophila* and surrogate microorganisms and compared the energy efficiency at  $3 \log_{10}$  inactivation with 254 nm LP UV, a WPE of 0.333 was applied for 254 nm LP while UV LEDs had lower values (0.006 for 265 nm, 0.019 for 280 nm, and 0.026 for 300 nm UV-LEDs, respectively). The results indicated higher energy efficiency using LP 254 nm which, was one to two orders of magnitude larger than those of UV LEDs, and 280 nm was the most effective among UV LEDs.<sup>83</sup> The higher electrical energy consumption of UV LEDs over LP due to the lower WPE was also indicated in a study disinfecting waterborne fungal spores.<sup>84</sup> For field applications of UV, the energy requirement for an optimized wastewater treatment process ranges from 0.057–0.172  $\text{kW h m}^{-3}$  and depends on many factors including the disinfection process, while the energy requirement for UV disinfection alone was 0.03  $\text{kW h m}^{-3}$ ,<sup>85</sup> which was at the same magnitude with our lab-scale study. The EEO requirement for treating chemicals in WWTPs was three orders of magnitude higher than the requirement for treating microorganisms.<sup>86,87</sup> The different energy requirements for field applications and chemical removal compared to lab scale cell inactivation and gene damage indicate areas of potential further exploration on the effects of energy consumption on factors including real water matrices such as dissolved organic matter, nitrate, and potential toxic by-products.

## 4. Conclusions

Our results indicated that 222 nm UV light exhibits higher efficacy over 254 nm in inactivating ARB, damaging intracellular ARG, and inhibiting HGT of ARB, and greater electrical efficiency of inhibiting HGT and competitive electrical efficiency of disinfecting ARB, suggesting 222 nm as a promising alternative or complement to existing disinfection for enhancing water treatment processes. Further explorations on other ARB and both plasmid and chromosomally encoded ARGs with multiple UV sources in various simulated and realistic water and wastewater treatment relevant matrices should be performed to optimize the UV efficiency or design protocols in engineered water systems.

## Data availability

The research data associated with the ARB UV disinfection study are available on the Figshare website (<https://figshare.com/account/home#/projects/210526>).

## Conflicts of interest

There are no conflicts to declare.

## Acknowledgements

This research was funded by startup support to Dr. Natalie Hull from the Department of Civil, Environmental, and Geodetic Engineering and the Sustainability Institute at The Ohio State University. I would also like to acknowledge Judith Straathof and Zanna Leciejewski for UV experiment training and Daniel Ma for help with troubleshooting.

## References

- 1 D. G. J. Larsson and C. F. Flach, *Nat. Rev. Microbiol.*, 2022, **20**, 257–269.
- 2 A. Pruden, R. Pei, H. Storteboom and K. H. Carlson, *Environ. Sci. Technol.*, 2006, **40**, 7445–7450.
- 3 P. J. Vikesland, A. Pruden, P. J. J. Alvarez, D. Aga, H. Bürgmann, X. Li, C. M. Manaia, I. Nambi, K. Wigginton, T. Zhang and Y.-G. Zhu, *Environ. Sci. Technol.*, 2017, **51**, 13061–13069.
- 4 C. U.S. Department of Health and Human Services, *Antibiotic resistance threats in the United States*, 2019, Atlanta, Georgia, 2019.
- 5 I. C. Stanton, A. Bethel, A. F. C. Leonard, W. H. Gaze and R. Garside, *Environ. Evid.*, 2022, **11**, 8.
- 6 N. G. Godijk, M. C. J. Bootsma and M. J. M. Bonten, *BMC Infect. Dis.*, 2022, **22**, 482.
- 7 P. De Voogt, *Reviews of Environmental Contamination and Toxicology*, 2015, vol. 236.
- 8 S. Bombaywala, A. Mandpe, S. Paliya and S. Kumar, *Environ. Sci. Pollut. Res.*, 2021, **28**, 24889–24916.
- 9 K. Liguori, I. Keenum, B. C. Davis, J. Calarco, E. Milligan, V. J. Harwood and A. Pruden, *Environ. Sci. Technol.*, 2022, **56**, 9149–9160.
- 10 J. Wang, L. Chu, L. Wojnárovits and E. Takács, *Sci. Total Environ.*, 2020, **744**, 140997.
- 11 S. Perveen, C. Pablos, K. Reynolds, S. Stanley and J. Marugán, *Sci. Total Environ.*, 2023, **856**, 159024.
- 12 E. Sanganyado and W. Gwenzi, *Sci. Total Environ.*, 2019, **669**, 785–797.
- 13 M. Kalli, C. Noutsopoulos and D. Mamais, *Water*, 2023, **15**(11), 2084.
- 14 M. Kang, J. Yang, S. Kim, J. Park, M. Kim and W. Park, *Sci. Total Environ.*, 2022, **811**, 152331.
- 15 T. Zhang, Y. Hu, L. Jiang, S. Yao, K. Lin, Y. Zhou and C. Cui, *Chem. Eng. J.*, 2019, **358**, 589–597.
- 16 H. Wang, J. Wang, S. Li, G. Ding, K. Wang, T. Zhuang, X. Huang and X. Wang, *Water Res.*, 2020, **185**, 116290.
- 17 A. K. Mittal, R. Bhardwaj, P. Mishra and S. K. Rajput, *Open Biotechnol. J.*, 2020, **14**, 107–112.



18 C. Bouki, D. Venieri and E. Diamadopoulos, *Ecotoxicol. Environ. Saf.*, 2013, **91**, 1–9.

19 J. Zheng, C. Su, J. Zhou, L. Xu, Y. Qian and H. Chen, *Chem. Eng. J.*, 2017, **317**, 309–316.

20 C. Li, F. Ling, M. Zhang, W. T. Liu, Y. Li and W. Liu, *J. Environ. Sci.*, 2017, **51**, 21–30.

21 O. M. Lee, H. Y. Kim, W. Park, T. H. Kim and S. Yu, *J. Hazard. Mater.*, 2015, **295**, 201–208.

22 P. Shi, S. Jia, X. X. Zhang, T. Zhang, S. Cheng and A. Li, *Water Res.*, 2013, **47**, 111–120.

23 J. Zhang, W. Li, J. Chen, W. Qi, F. Wang and Y. Zhou, *Chemosphere*, 2018, **203**, 368–380.

24 C. Xi, Y. Zhang, C. F. Marrs, W. Ye, C. Simon, B. Foxman and J. Nriagu, *Appl. Environ. Microbiol.*, 2009, **75**, 5714–5718.

25 J. Oh, D. E. Salcedo, C. A. Medriano and S. Kim, *J. Environ. Sci.*, 2014, **26**, 1238–1242.

26 S. Li, B. S. Ondon, S. H. Ho, Q. Zhou and F. Li, *J. Water Process Eng.*, 2023, **53**, 103907.

27 Y. Shen, J. Luo, A. Di Cesare, N. Guo, S. Zou and Y. Yang, *Environ. Pollut.*, 2024, **345**, 123427.

28 K. Gopal, S. S. Tripathy, J. L. Bersillon and S. P. Dubey, *J. Hazard. Mater.*, 2007, **140**, 1–6.

29 T. Furukawa, A. Jikumaru, T. Ueno and K. Sei, *Water*, 2017, **9**, 1–9.

30 L. Shen, T. M. Griffith, P. O. Nyangaresi, Y. Qin, X. Pang, G. Chen, M. Li, Y. Lu and B. Zhang, *J. Hazard. Mater.*, 2020, **386**, 121968.

31 W. Lin, S. Li, S. Zhang and X. Yu, *Water Res.*, 2016, **91**, 331–338.

32 M. T. Guo, Q. Bin Yuan and J. Yang, *Chemosphere*, 2013, **93**, 2864–2868.

33 R. P. Sinha and D. P. Häder, *Photochem. Photobiol. Sci.*, 2002, **1**, 225–236.

34 M. Oliveira, P. Truchado, R. Cordero-García, M. I. Gil, M. A. Soler, A. Rancaño, F. García, A. Álvarez-Ordóñez and A. Allende, *Antibiotics*, 2023, **12**(2), 400.

35 M. Munir, K. Wong and I. Xagoraraki, *Water Res.*, 2011, **45**, 681–693.

36 E. A. Auerbach, E. E. Seyfried and K. D. McMahon, *Water Res.*, 2007, **41**, 1143–1151.

37 M. T. Guo and C. Kong, *Chemosphere*, 2019, **224**, 827–832.

38 C. W. McKinney and A. Pruden, *Environ. Sci. Technol.*, 2012, **46**, 13393–13400.

39 W. Ben, L. Liu, Y. Gao, Z. Sun, J. Li and Z. Qiang, *ACS ES&T Water*, 2024, **4**(4), 1680–1687.

40 E. R. Blatchley, D. J. Brenner, H. Claus, T. E. Cowan, K. G. Linden, Y. Liu, T. Mao, S.-J. Park, P. J. Piper, R. M. Simons and D. H. Sliney, *Crit. Rev. Environ. Sci. Technol.*, 2022, 1–21.

41 J. Xu and C. Huang, *Environ. Sci. Technol. Lett.*, 2023, **10**(6), 543–548.

42 D. Wang, T. Oppenländer, M. G. El-Din and J. R. Bolton, *Photochem. Photobiol.*, 2010, **86**, 176–181.

43 H. He, P. Zhou, K. K. Shimabuku, X. Fang, S. Li, Y. Lee and M. C. Dodd, *Environ. Sci. Technol.*, 2019, **53**, 2013–2026.

44 H. Ul Haq, W. Huang, Y. Li, T. Zhang, S. Ma, Y. Zhang, Y. Song, D. Lin and B. Tian, *Biologia*, 2022, **77**, 1151–1160.

45 A. M. Earl, R. Losick and R. Kolter, *Trends Microbiol.*, 2008, **16**, 269–275.

46 N. Fluman and E. Bibi, *Biochim. Biophys. Acta, Proteins Proteomics*, 2009, **1794**, 738–747.

47 N. M. Hull, A. L. Reens, C. E. Robertson, L. F. Stanish, J. K. Harris, M. J. Stevens, D. N. Frank, C. Kotter and N. R. Pace, *Water Res.*, 2015, **69**, 318–327.

48 J. R. Bolton and K. G. Linden, *J. Environ. Eng.*, 2003, **129**, 209–215.

49 K. G. Linden and J. L. Darby, *J. Environ. Eng.*, 1997, **123**, 1142–1149.

50 D. Ma and N. Hull, *Polychromatic UV Fluence (Dose) Response Determination V.4*, *protocols.io*, 2024, DOI: [10.17504/protocols.io.n92ldzqoov5b/v4](https://doi.org/10.17504/protocols.io.n92ldzqoov5b/v4).

51 K. Sholtes and K. G. Linden, *Water Res.*, 2019, **165**, 114965.

52 S. E. Beck, H. Ryu, L. A. Boczek, J. L. Cashdollar, K. M. Jeanis, J. S. Rosenblum, O. R. Lawal and K. G. Linden, *Water Res.*, 2017, **109**, 207–216.

53 N. M. Hull and K. G. Linden, *Water Res.*, 2018, **143**, 292–300.

54 EPA, *Environmental Protection*, 2006, **2**, 1–436.

55 W. Taylor, E. Camilleri, D. L. Craft, G. Korza, M. R. Granados, J. Peterson, R. Szczeniak, S. K. Weller, R. Moeller, T. Douki, W. W. K. Mok and P. Setlow, *Appl. Environ. Microbiol.*, 2020, **86**, e03039-19.

56 K. Narita, K. Asano, K. Naito, H. Ohashi, M. Sasaki, Y. Morimoto, T. Igarashi and A. Nakane, *J. Hosp. Infect.*, 2020, **105**, 459–467.

57 T. Li, Y. Zhang, J. Gan, X. Yu and L. Wang, *J. Hazard. Mater.*, 2023, **452**, 131292.

58 A. C. Eischeid and K. G. Linden, *Appl. Environ. Microbiol.*, 2011, **77**, 1145–1147.

59 S. E. Beck, R. A. Rodriguez, K. G. Linden, T. M. Hargy, T. C. Larason and H. B. Wright, *Environ. Sci. Technol.*, 2014, **48**, 591–598.

60 R. S. N. Tavares, D. Adamoski, A. Girasole, E. N. Lima, A. da Silva Justo-Junior, R. Domingues, A. C. C. Silveira, R. E. Marques, M. de Carvalho, A. L. B. Ambrosio, A. F. P. Leme and S. M. G. Dias, *J. Photochem. Photobiol. B*, 2023, **243**, 112713.

61 Z. Jing, Z. Lu, D. Santoro, Z. Zhao, Y. Huang, Y. Ke, X. Wang and W. Sun, *Chem. Eng. J.*, 2022, **447**, 137584.

62 B. Ma, K. Bright, L. Ikner, C. Ley, S. Seyedi, C. P. Gerba, M. D. Sobsey, P. Piper and K. G. Linden, *Photochem. Photobiol.*, 2022, **99**, 975–982.

63 Z. Yang, P. Liu, H. Wei, H. Li, J. Li, X. Qiu, R. Ding and X. Guo, *Sci. Total Environ.*, 2022, **825**, 153918.

64 R. Destiani and M. R. Templeton, *AIMS Environ. Sci.*, 2019, **6**, 222–241.

65 M. F. Dias, G. da Rocha Fernandes, M. Cristina de Paiva, A. Christina de Matos Salim, A. B. Santos and A. M. Amaral Nascimento, *Water Res.*, 2020, **174**, 115630.

66 A. C. Lorenzo-Leal, W. Tam, A. Kheyrandish, M. Mohseni and H. Bach, *BioMed Res. Int.*, 2023, **2023**, 1–8.

67 M. Nihemaiti, Y. Yoon, H. He, M. C. Dodd, J. P. Croué and Y. Lee, *Water Res.*, 2020, **182**, 1–11.

68 Y. Yoon, H. He, M. C. Dodd and Y. Lee, *Water Res.*, 2021, **202**, 117408.

69 Y. Yoon, M. C. Dodd and Y. Lee, *Environ. Sci.: Water Res. Technol.*, 2018, **4**, 1239–1251.

70 M. Umar, *Int. J. Environ. Res. Public Health*, 2022, **19**(3), 1636.

71 X. Meng, F. Li, L. Yi, M. Y. Dieketseng, X. Wang, L. Zhou and G. Zheng, *J. Hazard. Mater.*, 2022, **430**, 128502.

72 R. T. Robinson, N. Mahfooz, O. Rosas-Mejia, Y. Liu and N. M. Hull, *Sci. Rep.*, 2022, **12**, 1–10.

73 M. Pazda, J. Kumirska, P. Stepnowski and E. Mulkiewicz, *Sci. Total Environ.*, 2019, **697**, 134023.

74 N. F. Gray, *Ultraviolet Disinfection*, Elsevier, 2nd edn, 2013.

75 Z. Qiao, Y. Ye, P. H. Chang, D. Thirunarayanan and K. R. Wigginton, *Environ. Sci. Technol.*, 2018, **52**, 10408–10415.

76 Y. Yoon, H. J. Chung, D. Y. Wen Di, M. C. Dodd, H. G. Hur and Y. Lee, *Water Res.*, 2017, **123**, 783–793.

77 Y. Choi, H. He, M. C. Dodd and Y. Lee, *Environ. Sci. Technol.*, 2021, **55**, 2541–2552.

78 D. Das, A. Bordoloi, M. P. Achary, D. J. Caldwell and R. P. S. Suri, *Sci. Total Environ.*, 2022, **833**, 155205.

79 P. H. Chang, B. Juhrend, T. M. Olson, C. F. Marrs and K. R. Wigginton, *Environ. Sci. Technol.*, 2017, **51**, 6185–6192.

80 D. Li, Z. Feng, B. Zhou, H. Chen and R. Yuan, *Sci. Total Environ.*, 2022, **844**, 157162.

81 M. Kneissl, *III-Nitride Ultraviolet Emitters: Technology and Applications*, 2016, vol. 227.

82 V. Martino, K. Ochsner, P. Peters, D. H. Zitomer and B. K. Mayer, *Environ. Eng. Sci.*, 2021, **38**, 458–468.

83 S. Rattanakul and K. Oguma, *Water Res.*, 2018, **130**, 31–37.

84 Q. Wan, G. Wen, R. Cao, X. Xu, H. Zhao, K. Li, J. Wang and T. Huang, *Water Res.*, 2020, **173**, 115553.

85 P. Gikas, *J. Environ. Manage.*, 2017, **203**, 621–629.

86 K. M. S. Hansen and H. R. Andersen, *Int. J. Photoenergy*, 2012, **2012**, 1–9.

87 A. C. Mecha, M. S. Onyango, A. Ochieng and M. N. B. Momba, *Chemosphere*, 2017, **186**, 669–676.